

## **AN ACCURATE COMPLEX PERMITTIVITY METHOD FOR THIN DIELECTRIC MATERIALS**

**U. C. Hasar** <sup>†</sup>

Department of Electrical and Electronics Engineering  
Ataturk University  
Erzurum 25240, Turkey

**O. Simsek**

Department of Physics  
Ataturk University  
Erzurum, 25240, Turkey

**Abstract**—A promising microwave method has been proposed to accurately determine the complex permittivity of thin materials. The method uses amplitude-only scattering parameter measurements at one frequency for this purpose. It resolves the problems arising from any offset of the sample inside its cell in complex reflection scattering parameter measurements and from any uncertainty in sample thickness in transmission scattering parameter measurements. The method determines unique permittivity since, for thin samples, multi-valued trigonometric terms can be linearized. It uses higher order approximations to extract highly accurate permittivity values. It works very well in limited frequency-band applications or for dispersive materials since it is based upon point-by-point (or frequency-by-frequency) measurements. For validation of the method, we measured the complex permittivity of two thin polytetrafluoro-ethylene (PTFE) samples.

### **1. INTRODUCTION**

Material characterization is an important issue in many material production, processing, and management applications in agriculture,

---

Corresponding author: U. C. Hasar (ugurcem@atauni.edu.tr).

<sup>†</sup> Also with Department of Electrical and Computer Engineering, Binghamton University, Binghamton 13902, NY, USA.

food engineering, medical treatments, bioengineering, and the concrete industry [1]. In addition, microwave engineering requires precise knowledge on electromagnetic properties of materials at microwave frequencies since microwave communications are playing more and more important roles in military, industrial, and civilian life [1, 2]. For these reasons, various microwave techniques, each with its unique advantages and constraints [1], are introduced to characterize the electrical properties of materials.

Electrical characterization of thin materials is needed for several reasons. For instance, the dielectric constant of vegetation has a direct effect on radar backscatter measured by airborne and space-borne microwave sensors. A good understanding of the dielectric properties of vegetation leaves is vital for extraction of useful information from the remotely sensed data for earth resources monitoring and management [3]. Also, in the field of electronics, it has been a lasting key issue to evaluate the relative complex permittivity ( $\epsilon_r$ ) of thin dielectric materials such as high-density packaging (HDP) [4].

Permittivity measurements of thin materials can be performed by using non-destructive methods such as open-ended waveguide and coaxial methods [5, 6]. In order to accurately measure the  $\epsilon_r$  for these methods, samples with larger apertures should be prepared. Besides, the sample must be sufficiently thick so that the interaction of the electromagnetic field with the non-contacting boundaries or sample holder is negligible [3]. Furthermore, any bad contact present between the waveguide or coaxial aperture and the sample surface may degrade the accuracy of measurements [7]. Finally, for open-ended waveguides and coaxial probes with a lift-off distance, thin samples may sag and thus alter the theoretical computations [8].

Free-space methods, as another nondestructive method, do not require that the sample thickness is moderate. However, it suffers from the diffraction at the edges of the sample. In order to reduce this effect, the transverse dimensions (height and width) of the sample can be selected sufficiently large. However, for thin materials, such a solution may decrease the performance of measurements as a result of sagging. As another solution, spot focusing horn-lens antennas can be employed [9]. Nonetheless, the bandwidth of this antenna system is limited due to focusing nature of the lens. As a final solution, a calibration procedure which takes into account the diffraction effects can be incorporated to the measurement system [10, 11]. The accuracy of this approach, however, is not so high since the footstep of the propagation is relatively large if the sample is placed at far zone.

Resonant methods have much better accuracy and sensitivity than nonresonant methods [1]. They are generally applied to the

characterization of low-loss materials. In a recent study, it has been shown that they are also applicable to high-loss materials provided that very small samples are prepared or higher volume cavities are constructed [12], though a meticulous sample preparation is needed before measurements. In addition, for an analysis over a broad frequency band, a new measurement set-up (a cavity) must be made. This is not feasible from a practical point of view. Tunable resonators can be used for a wider frequency band analysis; nonetheless, they are expensive and an increase in the frequency bandwidth accompanies a decrease in the accuracy.

Due to their relative simplicity, nonresonant waveguide transmission/reflection methods are presently the most widely used broadband measurement techniques [13]. These methods have effectively been applied to determine the  $\epsilon_r$  of thin materials [3, 7, 14–16]. It is not generally possible to locate thin samples to completely fill a coaxial line or rectangular waveguide section. In this circumstance, the transformation of scattering ( $S$ -) parameters from the calibration plane to the sample end surfaces (measurement plane) has to be done [17]. Such a transformation may result in enormous errors for phase measurement of reflection  $S$ -parameters. On the other hand, transmission  $S$ -parameter measurements are not affected if both the sample length and the sample holder length are known [7, 14, 15]. This is because transmission measurements take longitudinal averaging of variations in sample properties [18]. To overcome the problems arising from reflection  $S$ -parameters, transmission-only measurements can be employed [4, 18]. Although the method in [16] does not require complete filling of the cross section of a waveguide section, it requires adequate sample thickness in order to obtain accurate measurement result. As a solution to this problem, a transmission-only waveguide method can be utilized [3]. Although the derivations are independent upon any offset of the sample inside its holder, it is sensitive to sample thickness. As another solution to the measurement errors arising from reflection  $S$ -parameters, we have lately proposed various amplitude-only methods [19–23]. In this paper, we employ this new methodology to thin dielectric materials. The proposed method uses amplitudes of reflection and transmission properties of materials under test. The proposed method has three main features. First, it eliminates measurement errors arising from phase of reflection  $S$ -parameters. Second, it decreases any errors arising from inaccurately measured sample thickness for samples located at an offset from the calibration plane. Finally, it allows for easily positioning the sample inside a measurement cell greater in thickness than the sample. This, in turn, permits flexibility in measurements.

## 2. DIELECTRIC CONSTANT THEORY DEVELOPMENT

The problem for  $\varepsilon_r$  measurement of a thin material with length  $L$  inside a waveguide sample holder is depicted in Fig. 1. In the analysis, it is assumed that the sample is isotropic, symmetric and homogenous.

The expressions of electric and magnetic fields can be derived from their vector potentials (or hertzian vectors),  $\vec{A}$  and  $\vec{F}$ , such as [24]

$$\vec{E} = -j\omega\vec{A} - j\frac{1}{\omega\mu\varepsilon}\nabla(\nabla\cdot\vec{A}) - \frac{1}{\varepsilon}\nabla\times\vec{F} \quad (1)$$

$$\vec{H} = \frac{1}{\mu}\nabla\times\vec{A} - j\omega\vec{F} - j\frac{1}{\omega\mu\varepsilon}\nabla(\nabla\cdot\vec{F}). \quad (2)$$

Assuming that the rectangular waveguide operates in the dominant mode (TE<sub>10</sub>), we have  $\vec{A} = 0$  and  $\partial F_z/\partial y = 0$  [24]. Then, the electric vector potential can be written for regions I, II, and III as

$$F_z^{(I)}(x, z) = \cos\left(\frac{2\pi}{\lambda_c}x\right) [C_1e^{-\gamma_0 z} + C_2e^{\gamma_0 z}], \quad (3)$$

$$F_z^{(II)}(x, z) = \cos\left(\frac{2\pi}{\lambda_c}x\right) [C_3e^{-\gamma z} + C_4e^{\gamma z}], \quad (4)$$

$$F_z^{(III)}(x, z) = \cos\left(\frac{2\pi}{\lambda_c}x\right) C_5e^{-\gamma_0 z}, \quad (5)$$

where

$$\gamma_0 = j2\pi/\lambda_0\sqrt{1 - \lambda_0^2/\lambda_c^2}, \quad \gamma = j2\pi/\lambda_0\sqrt{\varepsilon_r - \lambda_0^2/\lambda_c^2}. \quad (6)$$

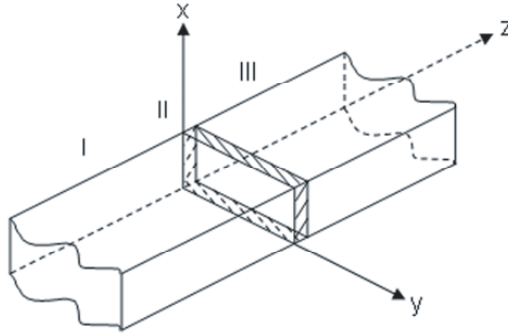


**Figure 1.** Illustration of the problem: Permittivity determination of thin materials inside rectangular waveguides.

Here,  $C_1 : C_5$  are the complex values;  $\lambda_0 = c/f$  and  $\lambda_c = c/f_c$  correspond to the free-space and cut-off wavelengths; and  $f$ ,  $f_c$ , and  $c$  are the operating and cut-off frequencies and the speed of light, respectively; and  $\varepsilon_r = \varepsilon'_r - j\varepsilon''_r$  is the relative complex permittivity of the sample.

Using the electric vector potentials in (3)–(5), electric and magnetic fields can be determined from (1) and (2). Applying boundary conditions at interfaces I-II and II-III ( $z = 0$  and  $z = L$ ),  $S$ -parameters can be derived as [13, 19, 20]

$$S_{11} = |S_{11}|e^{j\theta_{11}} = R_1^2\Gamma\frac{(1-T^2)}{1-\Gamma^2T^2}, \quad (7)$$

$$S_{22} = |S_{22}|e^{j\theta_{22}} = R_2^2\Gamma\frac{(1-T^2)}{1-\Gamma^2T^2}, \quad (8)$$

$$S_{21} = |S_{21}|e^{j\theta_{21}} = S_{12} = R_1R_2T\frac{(1-\Gamma^2)}{1-\Gamma^2T^2}, \quad (9)$$

where  $|\bullet|$  denotes the magnitude of expressions;  $\Gamma$  and  $T$  are, respectively, the reflection coefficient when the sample is infinite in length and the propagation factor; and  $R_1$  and  $R_2$  are the calibration plane transformation factors. Their corresponding equations are

$$\Gamma = \frac{\gamma_0 - \gamma}{\gamma_0 + \gamma}, \quad T = \exp(-\gamma L), \quad (10)$$

$$R_1 = \exp(-\gamma_0 L_1), \quad R_2 = \exp(-\gamma_0 L_2), \quad (11)$$

where  $L_1$  and  $L_2$  are the distances between the calibration plane and the sample end surfaces.

### 3. COMPLEX PERMITTIVITY DETERMINATION

In this section, we will derive some useful expressions for  $\varepsilon_r$  determination of thin materials using amplitude-only  $S$ -parameter measurements. It is clear that  $|S_{11}| = |S_{22}|$  from (7) and (8). Introducing the following new variables

$$\chi - j\xi = \sqrt{\varepsilon_r - (\lambda_0/\lambda_c)^2}, \quad B = \exp(-4\pi\xi L/\lambda_0), \quad (12)$$

$$A = 4\pi\chi L/\lambda_0, \quad \kappa = \sqrt{1 - (\lambda_0/\lambda_c)^2}, \quad (13)$$

into (7) and (9), we obtain [19, 20, 22]

$$|S_{11}| = \sqrt{(\Lambda_1^2 + \Lambda_2)(1 + B^2 - 2B \cos(A))/\psi}, \quad (14)$$

$$|S_{21}| = \sqrt{16B(\chi^2 + \xi^2)\kappa^2/\psi}, \quad (15)$$

where

$$\begin{aligned}\psi &= B^2\Lambda_3^2 + \Lambda_4^2 + 8\kappa\xi B \sin(A)\Lambda_1 - 2B \cos(A)(\Lambda_1^2 - \Lambda_2), \\ \Lambda_1 &= \chi^2 + \xi^2 - \kappa^2, \quad \Lambda_2 = 4\kappa^2\xi^2, \\ \Lambda_3 &= (\chi - \kappa)^2 + \xi^2, \quad \Lambda_4 = (\chi + \kappa)^2 + \xi^2.\end{aligned}\quad (16)$$

The definition of new variables changed the inverse problem from  $\varepsilon_r$  determination into  $\chi$  and  $\xi$  determination. Using (12) and (13), we obtain [19, 20]

$$\chi\xi = 0.5\varepsilon_r'', \quad \chi^2 = (\varepsilon_r' - 1) + \xi^2 + \kappa^2, \quad (17)$$

where  $0 < \kappa < 1$  for  $\lambda_0 < \lambda_c$ . For a passive medium, it is obvious that  $|T|$  must decrease with  $\varepsilon_r''$ . This condition enforces that  $\chi$  and  $\xi$  be real and greater than zero [19, 20].

Dividing (14) to (15), we obtain a objective function for  $\varepsilon_r$  measurement of thin materials as

$$\cos(A) = \frac{B + 1/B - \phi(\chi^2 + \xi^2)/(\Lambda_1^2 + \Lambda_2)}{2}, \quad \phi = \frac{16\kappa^2|S_{11}|^2}{|S_{21}|^2}. \quad (18)$$

For thin materials, we can approximate  $k_0\chi L \ll 1$  and  $C = k_0\xi L \ll 1$ . With these conditions at hand, we obtain

$$\cos A = 1 + f(A)/2, \quad (19)$$

$$B + 1/B = 2 + 4C^2 + 4C^4/3, \quad (20)$$

where

$$f(A) = -\frac{1}{2}A^2 + \frac{1}{24}A^4 - \frac{1}{720}A^6 + \frac{1}{40320}A^8 + \dots \quad (21)$$

Introducing the approximations in (19)–(21) into (18), we derive a relation between  $\chi$  and  $\xi$  as

$$f(\xi) = \xi^8 + \alpha_3\xi^6 + \alpha_2\xi^4 + \alpha_1\xi^2 + \alpha_0 = 0, \quad (22)$$

where

$$\alpha_3 = 2(\chi^2 + \kappa^2) + \frac{3}{k_0^2L^2}, \quad (23)$$

$$\alpha_2 = (\chi^2 - \kappa^2)^2 + \frac{6}{k_0^2L^2}(\chi^2 + \kappa^2) - \frac{3f(A)}{4k_0^4L^4}, \quad (24)$$

$$\alpha_1 = \frac{3}{k_0^2L^2}(\chi^2 - \kappa^2)^2 - \frac{3f(A)}{2k_0^4L^4}(\chi^2 + \kappa^2) - \frac{3\phi}{4k_0^4L^4}, \quad (25)$$

$$\alpha_0 = -\frac{3f(A)}{4k_0^4L^4}(\chi^2 - \kappa^2)^2 - \frac{3\phi}{4k_0^4L^4}\chi^2. \quad (26)$$

Therefore, the four roots of  $\xi$  from (22) will be [25]

$$\xi_{(1,2)} = \sqrt{-\frac{1}{4}\alpha_3 + \frac{1}{2}R \mp \frac{1}{2}D}, \quad \xi_{(3,4)} = \sqrt{-\frac{1}{4}\alpha_3 - \frac{1}{2}R \mp \frac{1}{2}E}, \quad (27)$$

where

$$R = \sqrt{\frac{1}{4}\alpha_3^2 - \alpha_2 + Y}, \quad (28)$$

$$D = \begin{cases} \sqrt{\frac{3}{4}\alpha_3^2 - R^2 - 2\alpha_2 + \frac{(4\alpha_3\alpha_2 - 8\alpha_1 - \alpha_3^3)}{4R}} & \text{for } R \neq 0 \\ \sqrt{\frac{3}{4}\alpha_3^2 - 2\alpha_2 + 2\sqrt{Y^2 - 4\alpha_0}} & \text{for } R = 0 \end{cases}, \quad (29)$$

$$E = \begin{cases} \sqrt{\frac{3}{4}\alpha_3^2 - R^2 - 2\alpha_2 - \frac{(4\alpha_3\alpha_2 - 8\alpha_1 - \alpha_3^3)}{4R}} & \text{for } R \neq 0 \\ \sqrt{\frac{3}{4}\alpha_3^2 - 2\alpha_2 - 2\sqrt{Y^2 - 4\alpha_0}} & \text{for } R = 0 \end{cases}, \quad (30)$$

$$Y = \left[ \frac{1}{2}Q + \sqrt{\frac{Q^2}{4} + \frac{P^3}{27}} \right]^{1/3} + \left[ \frac{1}{2}Q - \sqrt{\frac{Q^2}{4} + \frac{P^3}{27}} \right]^{1/3} - S, \quad (31)$$

$$Q = \frac{2}{27}\alpha_2^3 - \frac{1}{3}\alpha_2(\alpha_1\alpha_3 - 4\alpha_0) - (4\alpha_0\alpha_2 - \alpha_1^2 - \alpha_0\alpha_3^2), \quad (32)$$

$$P = (\alpha_1\alpha_3 - 4\alpha_0) - \frac{1}{3}\alpha_2^2, \quad S = -\frac{\alpha_2}{3}. \quad (33)$$

In (31), the roots of  $Y$  are

$$Y^3 - \alpha_2 Y^2 + (\alpha_1\alpha_3 - 4\alpha_0)Y + (4\alpha_0\alpha_2 - \alpha_1^2 - \alpha_0\alpha_3^2) = 0. \quad (34)$$

Since  $\chi$  and  $\xi$  are real and greater than zero [19, 20], only the real root must be selected from (27). After performing some computations with various test parameters of  $\varepsilon_r$ ,  $f$ ,  $f_c$  and  $L$ , we observed that only one of the roots of  $\xi$  yields a real solution. This is because the transcendental terms, which produce multiple solutions [19, 20], can be linearized for small  $k_0\chi L$  values. We also validated this conclusion by using the 'roots' function of MATLAB.

After determining  $\xi$  from (27),  $\chi$  can be computed by using any 1-D root searching algorithm [26]. This facilitates fast  $\varepsilon_r$  computations using the computed  $\xi$  and  $\chi$  values and Eq. (12). While our method relies on computation of  $\varepsilon_r$ , those in [3, 14] measure the  $\varepsilon_r$  noniteratively. However, it is expected that we will determine accurate  $\varepsilon_r$  values by using our method since we only use approximations in (19)–(21) for expressing  $\xi$  in terms of  $\chi$  and consider higher approximations for variables in (18). In addition, using the objective function in (18), even highly accurate results can be attained by

increasing the degree of the approximations in (19)–(21) and using ‘roots’ function of MATLAB.

#### 4. COMPUTATIONS FOR ASSESSING THE ACCURACY

In this section, our purpose is to compare the accuracy of  $\varepsilon_r$  measurements by different methods for various cases. We have used the same test parameters used in the paper [3] for the comparison. For example, Figs. 2 and 3 demonstrate the dependency of  $\varepsilon_r$  of a low-loss sample ( $\varepsilon_r = 2 - j0.05$ ) and a lossy sample ( $\varepsilon_r = 20 - j10$ ) versus the sample length using ‘roots’ function of MATLAB for the expression in (22). The test parameters are  $f = 5$  GHz and  $f_c = 3.152$  GHz (a C-band waveguide).

It is seen from Figs. 2 and 3 that while the reflection method [14] and the transmission method [3] extract similar results for  $\varepsilon_r$ , our proposed method yields very accurate results even at moderate sample lengths. We expect that our proposed method will determine much better  $\varepsilon_r$  values than the reflection and transmission methods [3, 14] at larger sample lengths. This can easily be deduced from the dependency in Fig. 3 since an increase in  $\varepsilon_r'$  and  $\varepsilon_r''$  corresponds to an increase in  $L$  for the same sample length range.

Since reflection measurements depend highly on the offset of the sample inside its holder and the proposed transmission method in [3] depends considerably upon the sample length, we compared our method with these methods while these uncertainty makers are present. For example, Figs. 4 and 5 illustrate the dependency of  $\varepsilon_r$  for the same test samples in Figs. 2 and 3 versus the sample length. It is assumed that only a 0.5 mm sample offset is present in the reflection measurement [14] while the phase shift from the calibration plane in transmission measurements in [3] arises from an uncertainty corresponding to a 1 percent offset in the sample length.

It is seen in Figs. 4 and 5 that when the sample position offset and the uncertainty in sample length measurement are present, the reflection and transmission methods in [3] and [14] will yield inaccurate results especially for the  $\varepsilon_r''$ . However, our proposed method results in accurate values for both real and imaginary parts of  $\varepsilon_r$ . Besides, whereas the reflection and transmission methods in [3] and [14] will be affected by errors in calibration planes, our proposed method does not. This is because it is based on amplitude-only measurements.

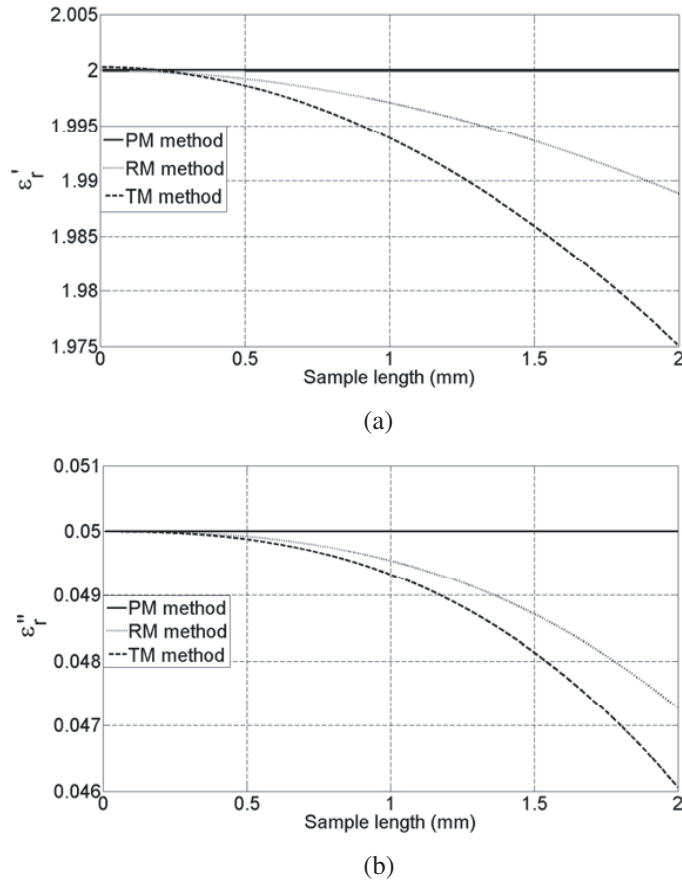


**Figure 2.** Dependency of relative dielectric constant (a) real part, and (b) imaginary part of a lowloss material ( $\epsilon_r = 2 - j0.05$ ) versus sample length. In the figure, PM, RM and TM, respectively, denote the proposed method, the reflection method [14] and the transmission method [3].

## 5. MEASUREMENT RESULTS

A general purpose waveguide measurement set-up is used for validation of the proposed method [19]. A HP8720C VNA is connected as a source and measurement equipment. It has a 1 Hz frequency resolution (with option 001) and 8 ppm (parts per million) frequency accuracy. The waveguide used in measurements has a width of  $22.86 \pm 5\%$  mm ( $f_c \cong 6.555$  GHz). We employed two extra waveguide sections with

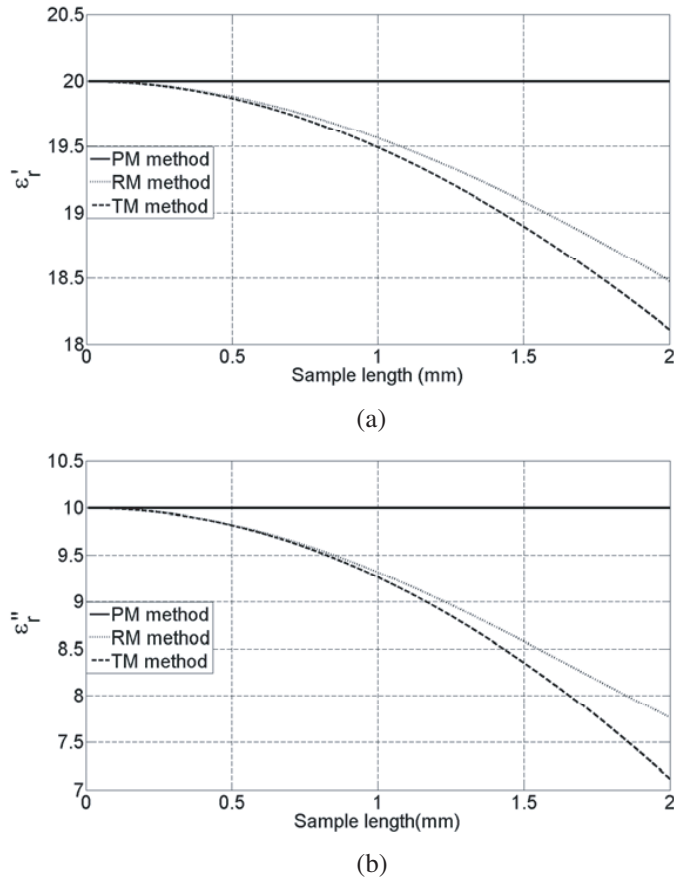


**Figure 3.** Dependency of relative dielectric constant (a) real part, and (b) imaginary part of a lowloss material ( $\epsilon_r = 20 - j10$ ) versus sample length. In the figure, PM, RM and TM, respectively, denote the proposed method, the reflection method [14] and the transmission method [3].

lengths greater than  $2\lambda_0$  at X-band between the calibration (reference) plane and coaxial-to-waveguide adapters to filter out any higher order modes [27].

The thru-reflect-line (TRL) calibration technique [28] is utilized before measurements. We used a waveguide with the shortest waveguide spacer ( $44.38 \mp 5\%$  mm) in our lab for reflection and line standards, respectively. The line has a  $\pm 70^\circ$  maximum offset from  $90^\circ$  between 9.7 GHz and 11.7 GHz. After calibration of the set-up, we paid

special attention to preparing 2 mm and 3 mm long polytetrafluoroethylene (PTFE) samples with no scratches, nicks, or cracks [27]. We machined the samples so that they fit precisely into the line standard to reduce the air gaps between their external surfaces and the holder [27].

Several factors contribute to the uncertainty in  $\epsilon_r$  determination in waveguide measurements [13, 27] namely: 1) the uncertainty in measured  $S$ -parameters; 2) errors in the sample length and the holder

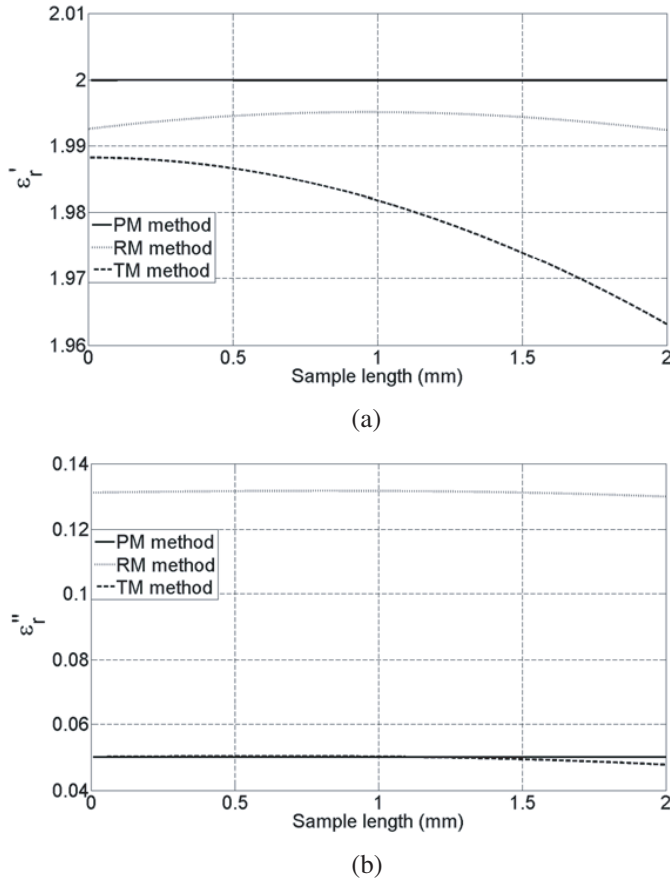


**Figure 4.** Dependency of relative dielectric constant (a) real part, and (b) imaginary part of a lowloss material ( $\epsilon_r = 2 - j0.05$ ) versus sample length when there is a 0.5 mm offset in sample position and phase uncertainty arising from a 1 percent offset in the sample length in the transmission measurement [3]. In the figure, PM, RM and TM, respectively, denote the proposed method, the reflection method [14] and the transmission method [3].

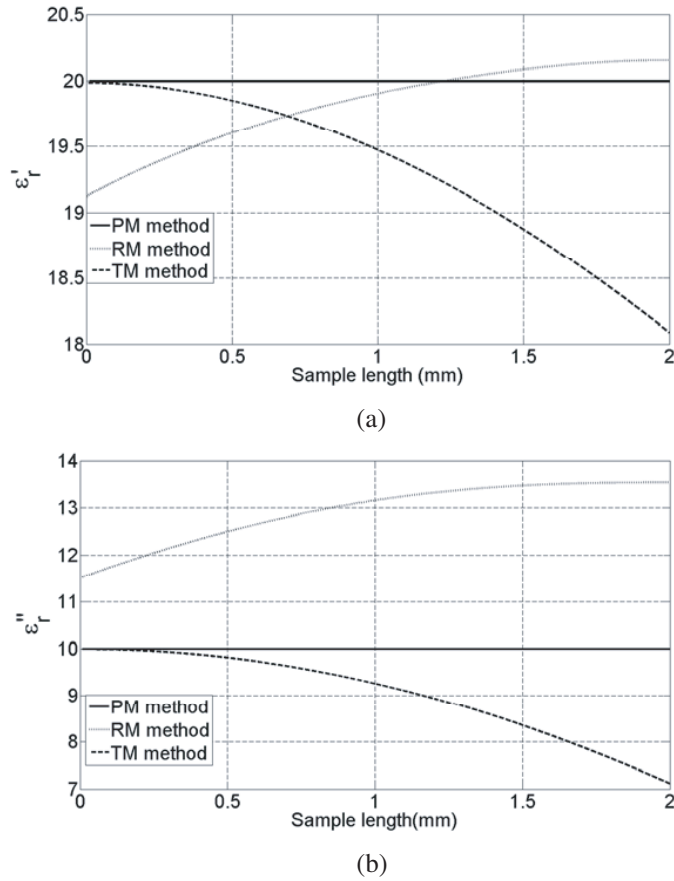


**Figure 5.** Dependency of relative dielectric constant (a) real part, and (b) imaginary part of a lowloss material ( $\epsilon_r = 20 - j10$ ) versus sample length when there is a 0.5 mm offset in sample position and phase uncertainty arising from a 1 percent offset in the sample length in the transmission measurement [3]. In the figure, PM, RM and TM, respectively, denote the proposed method, the reflection method [14] and the transmission method [3].

length; 3) the uncertainty in reference plane positions; 4) guide losses and conductor mismatches; 5) air gaps between the external surfaces of the sample (and holder) and inner walls of waveguides; and 6) higher order modes. All these uncertainties are extensively treated in the literature [13, 27]. Here, our attention is to analyze the uncertainty arising from  $S$ -parameters. It was shown that the phase uncertainty

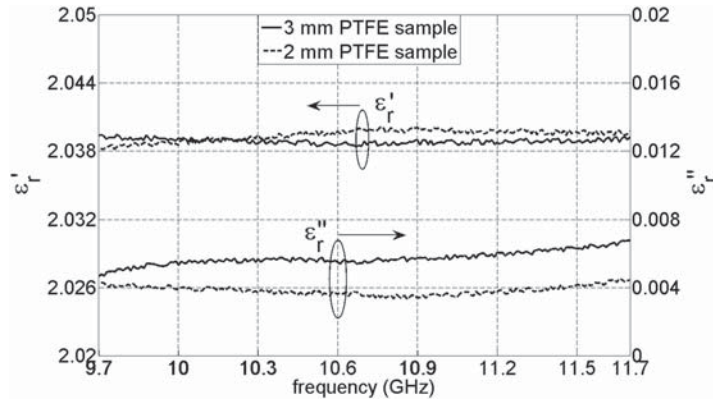


**Figure 6.** Measured relative complex permittivity of 2 mm and 3 mm long PTFE samples by the proposed method.

in the measured  $S_{11}$  greatly increases when  $\cos(A) \cong 1$  in (18) [19]. It is seen from (18) that, for very thin samples, it is very less likely to observe large phase uncertainties in the measured  $S_{11}$  over a small frequency range. Whether the phase uncertainty in  $S_{11}$  considerably increases or not, our proposed method resolves the problems arising from this uncertainty and any offset in sample position inside its cell since it utilizes amplitude-only measurements. Besides, for very thin samples, the attenuation of wave propagation through the sample will be low (less than approximately  $-30$  dB). Thus, we expect that the measured amplitude of  $S_{21}$  is highly accurate, which demonstrates the efficacy and potential of the proposed method.

We positioned the samples into the line standard and then collected 801 data points evenly spaced between 9.7 GHz and 11.7 GHz. Next, we applied the time-domain gating over the main transmission properties of the samples to decrease post reflections, which may arise after the TRL calibration, and to obtain smoother  $S$ -parameter measurements [9]. For example, Fig. 6 demonstrates the extracted  $\epsilon_r$  of the PTFE samples. Although numerical methods generally require a good initial guess for convergence, in the  $\epsilon_r$  determination by our method, we did not utilize any special information for the range of  $\epsilon_r$ . All we assume for every sample is  $\chi \geq 1$  and  $\xi \geq 0$ , which are obtained from (12) and (17).

It is seen from Fig. 6 that there is a good agreement between the measured spectral data of PTFE samples and the measurements in [3] and the published data in the literature [29]. At 10 GHz, the  $\epsilon_r$  of the PTFE sample given by Von Hippel is  $2.08 - j0.00076$  [29].

## 6. CONCLUSION

An effective method is developed for complex permittivity of thin materials positioned into its cell. The method solely uses amplitude-only scattering parameter measurements in order to resolve the problems arising from any offset of the sample inside its cell and reduce the uncertainty in sample thickness. The method approximates the multi-valued trigonometric terms, which produce multiple solutions for complex permittivity extraction, to simple expressions for thin samples for unique permittivity measurements. The method extracts the permittivity from point-by-point (or frequency-by-frequency) measurements. Therefore, it is applicable to band-limited applications.

## ACKNOWLEDGMENT

U. C. Hasar (Mehmetcik) would like to thank TUBITAK (The Scientific and Technological Research Council of Turkey) Mnrir Birsol National Doctorate Scholarship and YOK (The Higher Education Council of Turkey) Doctorate Scholarship for supporting his studies.

## REFERENCES

1. Chen, L. F., C. K. Ong, C. P. Neo, et al., *Microwave Electronics: Measurement and Materials Characterization*, John Wiley & Sons, West Sussex, England, 2004.
2. Hebeish, A. A., M. A. Elgamel, R. A. Abdelhady, et al., "Factors affecting the performance of the radar absorbant textile materials of different types and structures," *Progress In Electromagnetics Research B*, Vol. 3, 219–226, 2008.
3. Chung, B.-K., "Dielectric constant measurement for thin material at microwave frequencies," *Progress In Electromagnetics Research*, PIER 75, 239–252, 2007.
4. Murata, K., A. Hanawa, and R. Nozaki, "Broadband complex permittivity measurement techniques of materials with thin configuration at microwave frequencies," *J. Applied Phys.*, Vol. 98, 084107-1–084107-08, 2005.
5. Decreton, M. C. and F. E. Gardiol, "Simple non-destructive method for the measurement of complex permittivity," *IEEE Trans. Instrum. Meas.*, Vol. 23, 434–438, 1974.
6. Zhang, H., S. Y. Tan, and H. S. Tan, "An improved method for microwave nondestructive dielectric measurement of layered

- media,” *Progress in Electromagnetics Research B*, Vol. 10, 145–161, 2008.
7. Olmi, R., M. Tedesco, C. Riminesi, et al., “Thickness-independent measurement of the permittivity of thin samples in the X band,” *Meas. Sci. Technol.*, Vol. 13, 503–509, 2002.
  8. Baker-Jarvis, J., M. D. Janezic, P. D. Domich, et al., “Analysis of an open-ended coaxial probe with lift-off for nondestructive testing,” *IEEE Trans. Instrum. Meas.*, Vol. 43, 711–718, 1994.
  9. Ghodgaonkar, D. K., V. V. Varadan, and V. K. Varadan, “Free-space measurement of complex permittivity and complex permeability of magnetic materials at microwave frequencies,” *IEEE Trans. Instrum. Meas.*, Vol. 39, 387–394, 1990.
  10. Hock, K. M., “Error correction for diffraction and multiple scattering in free-space microwave measurement of materials,” *IEEE Trans. Microw Theory Tech.*, Vol. 54, 648–659, 2006.
  11. Hasar, U. C., “A microcontroller-based microwave measurement system for permittivity determination of fresh cement-based materials,” *Proc. IEEE Instrumentation and Measurement Technology Conf. (IMTC’07)*, 2007.
  12. Rubinger, C. P. L. and L. C. Costa, “Building a resonant cavity for the measurement of microwave dielectric permittivity of high loss materials,” *Microwave Opt. Tech. Lett.*, Vol. 49, 1687–1690, 2007.
  13. Baker-Jarvis, J., E. J. Vanzura, and W. A. Kissick, “Improved technique for determining complex permittivity with the transmission/reflection method,” *IEEE Trans. Microw. Theory Tech.*, Vol. 38, 1096–1103, 1990.
  14. Sarabandi, K. and F. T. Ulaby, “Technique for measuring the dielectric constant of thin materials,” *IEEE Trans. Instrum. Meas.*, Vol. 37, 631–636, 1988.
  15. Kenneth, E. D. and L. J. Buckley, “Dielectric materials measurement of thin samples at millimeter wavelengths,” *IEEE Trans. Instrum. Meas.*, Vol. 41, 723–725, 1992.
  16. Chung, B.-K., “A convenient method for complex permittivity measurement of thin materials at microwave frequencies,” *J. Phys. D.: Appl. Phys.*, Vol. 39, 1926–1931, 2006.
  17. Challa, R. K., D. Kajfez, J. R. Gladden, et al., “Permittivity measurement with a non-standard waveguide by using TRL calibration and fractional linear data fitting,” *Progress In Electromagnetics Research B*, Vol. 2, 1–13, 2008.
  18. Ness, J., “Broad-band permittivity measurements using the semi-

- automatic network analyzer," *IEEE Trans. Microw. Theory Tech.*, Vol. 33, 1222–1226, 1985.
19. Hasar, U. C., "Two novel amplitude-only methods for complex permittivity determination of medium-and low-loss materials," *Meas. Sci. Technol.*, Vol. 19, 055706–055715, 2008.
  20. Hasar, U. C. and C. R. Westgate, "A broadband and stable method for unique complex permittivity determination of low-loss materials," *IEEE Trans. Microw. Theory Tech.*, Vol. 57, 471–477, 2009.
  21. Hasar, U. C., "A fast and accurate amplitude-only transmission reflection method for complex permittivity determination of lossy materials," *IEEE Trans. Microw. Theory Tech.*, Vol. 56, 2129–2135, 2008.
  22. Hasar, U. C., "Simple calibration plane-invariant method for complex permittivity determination of dispersive and non-dispersive low-loss materials," *IET Microw. Antennas Propag.*, 2009.
  23. Hasar, U. C., "Elimination of the multiple-solutions ambiguity in permittivity extraction from transmission-only measurements of lossy materials," *Microw. Opt. Technol. Lett.*, Vol. 51, 337–341, 2009.
  24. Balanis, C. A., *Advanced Engineering Electromagnetics*, John Wiley & Sons, New Jersey, NJ, 1989.
  25. Abramowitz, M. and I. A. Stegun (eds.), *Handbook of Mathematical Functions with Formulas, Graphs, and Mathematical Tables*, 17–18, Dover Publications, New York, NY, 1972.
  26. Press, W. H., S. A. Teukolsky, W. T. Vetterling, et al., *Numerical Recipes in C: The Art of Scientific Computing*, Ch. 9, Cambridge University Press, New York, NY, 1992.
  27. Baker-Jarvis, J., "Transmission/reflection and short-circuit line permittivity measurements" *Natl. Inst. Stand. Technol.*, 1341, Boulder, CO. Tech., July 1990.
  28. Engen, G. F. and C. A. Hoer, "Thru-reflect-line': An improved technique for calibrating the dual six-port automatic network analyzer," *IEEE Trans. Microw. Theory Tech.*, Vol. 27, 987–993, 1979.
  29. Von Hippel, A. R., *Dielectric Materials and Applications*, John Wiley & Sons, New York, NY, 1954.